Ankyrin-B Is Required for Intracellular Sorting of Structurally Diverse Ca^{2+} Homeostasis Proteins

Shmuel Tuvia, Mona Buhusi, Lydia Davis, Mary Reedy, and Vann Bennett

Howard Hughes Medical Institute and Departments of Cell Biology and Biochemistry, Duke University Medical Center, Durham, North Carolina 27710

Abstract. This report describes a congenital myopathy and major loss of thymic lymphocytes in ankyrin-B (−/−) mice as well as dramatic alterations in intracellular localization of key components of the Ca^{2+} homeostasis machinery in ankyrin-B (−/−) striated muscle and thymus. The sacoplasmic reticulum (SR) and SR/T-tubule junctions are apparently preserved in a normal distribution in ankyrin-B (−/−) skeletal muscle based on electron microscopy and the presence of a normal pattern of triadin and dihydropyridine receptor. Therefore, the abnormal localization of SR/ER Ca ATPase (SERCA) and ryanodine receptors represents a defect in intracellular sorting of these proteins in skeletal muscle. Extrapolation of these observations suggests defective targeting as the basis for abnormal localization of ryanodine receptors, IP3 receptors and SERCA in heart, and of IP3 receptors in the thymus of ankyrin-B (−/−) mice. Mis-sorting of SERCA 2 and ryanodine receptor 2 in ankyrin-B (−/−) cardiomyocytes is rescued by expression of 220-kD ankyrin-B, demonstrating that lack of the 220-kD ankyrin-B polypeptide is the primary defect in these cells. Ankyrin-B is associated with intracellular vesicles, but is not colocalized with the bulk of SERCA 1 or ryanodine receptor type 1 in skeletal muscle. These data provide the first evidence of a physiological requirement for ankyrin-B in intracellular targeting of the calcium homeostasis machinery of striated muscle and immune system, and moreover, support a catalytic role that does not involve permanent stoichiometric complexes between ankyrin-B and targeted proteins. Ankyrin-B is a member of a family of adapter proteins implicated in restriction of diverse proteins to specialized plasma membrane domains. Similar mechanisms involving ankyrins may be essential for segregation of functionally defined proteins within specialized regions of the plasma membrane and within the Ca^{2+} homeostasis compartment of the ER.

Key words: calcium homeostasis • IP3 receptor • ankyrin • sarcoplasmic reticulum • gene knockout

THE ER of metazoan cells is a continuous system of intracellular membranes segregated into subdomains with specialized functions (Vertel et al., 1992). One ER compartment with particular relevance for cell signaling is devoted to Ca^{2+} homeostasis, and is a major determinant of intracellular Ca^{2+} levels (Meldolesi and Pozzan, 1998). An ER Ca^{2+} homeostasis compartment is present in many cell types, but is morphologically best defined in striated muscle and the nervous system (Henkart et al., 1976; Franzini-Armstrong and Protasi, 1997; Berridge, 1998). The ER Ca^{2+} compartment of striated muscle, termed the sarcoplasmic reticulum (SR)[1], is intimately integrated with sarcomeres. In heart muscle, this configuration allows generation of Ca^{2+} waves that generate periodic cycles of contraction and relaxation by the contractile apparatus. Ryanodine receptors mediate Ca^{2+} release from SR stores, and are localized adjacent to voltage-sensitive Ca^{2+} channels in T-tubules, which are extensions of the plasma membrane (Franzini-Armstrong and Protasi, 1997). The SR/ER CaATPase (SERCA) is responsible for subsequent Ca^{2+} uptake into the SR lumen, and is localized over actomyosin in the A-band at sites distinct from ryanodine receptors (Jorgensen et al., 1993).

Little is known about how Ca^{2+} homeostasis proteins are targeted to specialized sites within the ER. Presumably, accessory proteins are required for segregation of functionally related but structurally distinct Ca^{2+} compartment proteins within the ER, for delivery of some of these proteins to the Golgi, and for subsequent sorting of proteins to specialized regions of the sarcoplasmic reticulum. Ankyrins are a family of membrane-associated adapter proteins (Bennett et al., 1997) that bind via their mem-

S. Tuvia and M. Buhusi contributed equally to this paper.

Address correspondence to Vann Bennett, Department of Biochemistry, Duke University Medical Center, 363 Carl Bldg., Res Drive, Box 3892, Durham, NC 27710-0001. Tel.: (919) 684-3538. Fax: (919) 684-3590. E-mail: benne012@mc.duke.edu

1. *Abbreviations used in this paper:* GFP, green fluorescent protein; SERCA, SR/ER Ca ATPase; SR, sarcoplasmic reticulum.

brane-binding domains to diverse proteins, including ryanodine receptors (Bourguignon et al., 1995) and IP3 receptors (Bourguignon et al., 1993). Ankyrins have been localized in striated muscle adjacent to voltage-sensitive Ca^{2+} channels in T-tubules (Flucher et al., 1990), and with SERCA in the SR (Zhou et al., 1997; Kordeli et al., 1998). Ankyrins are present in specialized plasma membrane domains, but also are associated with Golgi and other intracellular membranes (Devarajan et al., 1996; Beck et al., 1997; Hoock et al., 1997; Beck and Nelson, 1998; De Matteis and Morrow, 1998). 119-kD ankyrin-G colocalizes with the Golgi apparatus and participates in polarized delivery of Na/K ATPase to basolateral domains of epithelial cells (Devarajan et al., 1996, 1997). These considerations provide circumstantial support for a role of ankyrins in organization of proteins in several intracellular membrane systems including the SR of striated muscle.

Gene knockouts in mice have provided insight into physiological functions of the ankyrin family. Disruption of ankyrin-G expression in the cerebellum prevents restriction of voltage-gated sodium channels and L1CAM cell adhesion molecules to axon initial segments (Zhou et al., 1998). Knockout of the ankyrin-B gene was initially characterized in the nervous system, where the 440-kD ankyrin-B isoform is required for postnatal survival of premyelinated axons (Scotland et al., 1998).

This study reports that ankyrin-B is expressed in striated muscle and the thymus in addition to the nervous system of normal mice. Ankyrin-B (−/−) mice exhibit musculoskeletal defects, a major reduction in thymic lymphocytes, and the majority die on the first day after birth. Moreover, ryanodine receptors and SERCA are not distributed normally in ankyrin-B (−/−) striated muscle, and IP3 receptors are abnormally localized in ankyrin-B (−/−) thymic lymphocytes. These findings considered together with the requirement for ankyrin-G in targeting voltage-gated sodium channels to axon initial segments (Zhou et al., 1998), suggest that ankyrins function in related pathways required for targeting of functionally defined proteins to specialized domains in the plasma membrane and within the ER.

Materials and Methods

Materials

The following primary antibodies were used: affinity-purified rabbit anti-ankyrin-B (COOH terminus specific) polyclonal antibody (Scotland et al., 1998); monoclonal antibody against the dihydropyridine receptor, α2 subunit, (Affinity Bioreagents); SERCA, type 1 and 2 (Affinity Bioreagents); ryanodine receptor type 1 and 2 (Affinity Bioreagents); triadin (Affinity Bioreagents); IP3R (type 1, 2, and 3; Accurate Biochemicals); and sarcomere α-actinin (Sigma). Secondary antibodies used were: rhodamine- or fluorescein-conjugated goat anti–mouse IgG (Pierce and Jackson ImmunoResearch Laboratories) at 5 μg/ml and Cy-5- or rhodamine-conjugated goat anti–rabbit IgG (Jackson ImmunoResearch Laboratories) at 5 μg/ml. F-actin was visualized using biotin-phalloidin (5 U/ml; Molecular Probes) and Cy5-labeled streptavidin (Jackson ImmunoResearch Laboratories).

Procedures

Mouse genotypes were established by Southern blot analysis (Scotland et al., 1998), or by PCR. Tissue samples and cells were processed for SDS-PAGE/immunoblots and immunofluorescence and by laser scanning confocal microscopy as described in previous publications (Scotland et al., 1998; Zhou et al., 1998).

Neonatal Cardiomyocyte Culture and Transfection

Hearts were dissected from neonatal (1–3-d-old) mice under sterile conditions by bathing the animal in 70% alcohol. Each heart was then placed in a 12-well flat-bottom tissue culture plate containing 2 ml of Ham's F10 nutrient media. The atrium and major blood vessels were removed and the ventricle was rinsed by squeezing with forceps to wash away the blood. The ventricle was minced finely in 1.5 ml of 0.05% trypsin, 0.2 mM NaEDTA, and placed in a humidified incubator (37°C, 95% air-5% CO2) for 15 min. Ventricles were then resuspended several times in a 1-ml Eppendorf pipette and incubated for another 15 min. After incubation, 0.2 ml of 2-mg/ml soybean trypsin inhibitor was added, followed by the addition of 0.2 ml of 0.2-mg/ml collagenase (type VII; Sigma). The homogenate was resuspended several times and incubated further for 30–50 min until dissociation of cells was complete. Then 2 ml of complete media (DME/Ham's F10, 10% FBS, and 10% HS) was added, and cells were pelleted by centrifugation at 500 *g* for 5–10 min. Cells were resuspended in 2 ml complete media and transferred to a 35-mm petri dish to remove fibroblasts by differential adherence (2 h at 37°C). Cardiomyocytes in the supernatant were collected by centrifugation at 500 *g* for 5–10 min, and resuspended in 1 ml complete media. 0.25 ml of cell suspension were plated on a fibronectin-coated plate at a density of 1×10^6/ml and washed 24 h later with complete media to remove dead cells and debris. To minimize growth of nonmuscle cells, complete media was replaced with defined growth medium (DMEM/F10) with additions of insulin (1 μg/ml), transferrin (5 μg/ml), LiCl (1 nM), $NaSeO_4$ (1 nM), ascorbic acid (25 μg/ml), thyroxine (1 nm), or with serum-free medium (DMEM/F10). Cardiomyocytes were transfected using Effectene (Qiagen) with 0.1 μg of cDNA encoding 220-kD ankyrin-B or 190-kD ankyrin-G (Zhang and Bennett, 1998), both with EGFP positioned at the COOH termini of ankyrins in a pEGFP vector (Clontech).

Electron Microscopy

Quadriceps muscles from 7-d-old littermates were placed directly in Karnovsky glutaraldehyde/formaldehyde/cacodylate fixative plus tannic acid (pH 7.4) and sliced into smaller pieces (Nassar et al., 1987). After fixing for 3 h (room temperature) or overnight (4°C), pieces were thoroughly rinsed in MOPS buffered mammalian Ringer and further fixed in 0.2% tannic acid, 3% glutaraldehyde in MOPS buffered Ringer (pH 7.0) for 30 min. After rinsing in MOPS buffered Ringer, followed by 100 mM phosphate buffer, pH 6.1, tissue was post-fixed for 1 h in ice-cold 1% OsO4 in 100 mM potassium phosphate buffer, pH 6.1, rinsed in water, block stained in 2% aqueous uranyl acetate for 1 h, rinsed in water, dehydrated in a graded ethanol series, and embedded in Araldite 506 (Reedy and Reedy, 1985). Ultrathin sections were photographed at magnifications ranging from 3,800 to 18,500 on a Philips EM420 microscope.

Ca^{2+} Dynamics

Cytosolic Ca^{2+} levels were viewed in spontaneously contracting neonatal cardiomyocytes loaded with 10 μM fluo-3/AM (Molecular Probes) by ratioing fluo-3 images (excitation 488 nm, emission 510 nm) against a reference image acquired at rest (I/I_0) as described (Cheng et al., 1996). A 40× 1.2 NA water immersion objective was used and images were recorded at 6–12 frames/s. Data were analyzed using the LSM 410 data analysis software.

Creatine Kinase Activity

Creatine kinase activity in mouse serum was measured using a Sigma Diagnostics Creatine Kinase kit.

Fractionation of Skeletal Muscle

Fresh rat skeletal muscle samples were homogenized in a buffer (1 g/15 ml) containing 0.25 M sucrose, 100 mM Tris, pH 7.4, 5 mM sodium EDTA, 5 mM sodium EGTA, PMSF (200 μg/ml), leupeptin (10 μg/ml), AEBSF (0.5 mM), and pepstatin (10 μg/ml), centrifuged at 1,300 *g* for 10 min, rehomogenized and spun again. The supernatant was spun at 9,000 *g* for 10 min. The second supernatant was spun at 190,000 *g* for 1 h. Pellets were resuspended in 3 ml buffer and loaded on a 20–50% sucrose gradient, and

then centrifuged at 150,000 *g* for 16 h. Samples were treated as described above.

Results

Musculoskeletal Defects and Neonatal Myopathy in Ankyrin-B (−/−) Mice

Ankyrin-B (−/−) mice display abnormal posture with kyphosis and winged scapulae (Fig. 1 A). Creatine kinase activity also is elevated about fourfold in sera from ankyrin-B (−/−) mice compared with normal littermates, based on determinations of seven litters at ages ranging from postnatal day 1 to 13 (Fig. 1 B). Measurements of neonatal heterozygotes revealed some mice (8 out of 26) with a two- to threefold increase and other mice with normal levels of serum creatine kinase activity. For comparison, patients with congenital myopathies or mild muscular dystrophy frequently have normal levels or small elevation in levels of creatine kinase activity.

Transmission electron micrographs of ankyrin-B (−/−) heart (not shown) and skeletal muscle (Fig. 1 C) demonstrate overall normal sarcomere organization. However, occasional localized sites of severely disorganized sarcomeres and loss of striations encompassing 3–6 sarcomeres were observed in ankyrin-B (−/−) skeletal muscle (Fig. 1 C, yellow asterisk). Disorganized sarcomeres were not observed in skeletal muscle from normal littermates, and also were not evident in heart sections of either wild-type or ankyrin-B (−/−) mice (not shown).

Sites of disorganized sarcomeres, combined with elevation of serum creatine kinase activity and reduced myofibril size (not shown), support the conclusion that ankyrin-B (−/−) mice suffer from a neonatal myopathy and suggest a physiological role of ankyrin-B in muscle. Ankyrin-B polypeptides of 220 and 150 kD are expressed in skeletal muscle and heart of normal mice, and are not detectable in ankyrin-B (−/−) mice (Scotland et al., 1998; Fig. 1 D). Ankyrin-B (−/−) mice are born in Mendelian ratios, but suffer 70–80% mortality on postnatal day 1, and 100% by postnatal day 21. Causes of neonatal death are likely to include compromised function of striated muscle and the immune system (see below), in addition to previously described defects in the nervous system (Scotland et al., 1998).

Abnormal Ca^{2+} Waves and Mis-Sorting of Ca^{2+} Homeostasis Proteins in Ankyrin-B (−/−) Cardiomyocytes

Previous reports that ankyrin associates with IP3 receptors and ryanodine receptors (Bourguignon et al., 1993; 1995) suggested the possibility that Ca^{2+} homeostasis might be abnormal in ankyrin-B (−/−) mice. Dynamic patterns of intracellular Ca^{2+} release and uptake were measured in cardiomyocytes cultured from 1-d-old ankyrin-B (+/+) and (−/−) mice and maintained for 96 h, using Fluo-3 as an indicator (Fig. 2). Ankyrin-B (+/+) and (−/−) cardiomyocytes in these cultures spontaneously contract, and have assembled sarcomeres and T-tubules, based on patterns of fluorescent labeling of α-actinin (Fig. 3 A1), F-actin (Fig. 4, A–H, left panels), and voltage-gated calcium channels (Fig. 3 C). Normal cardiomyocytes exhibit a

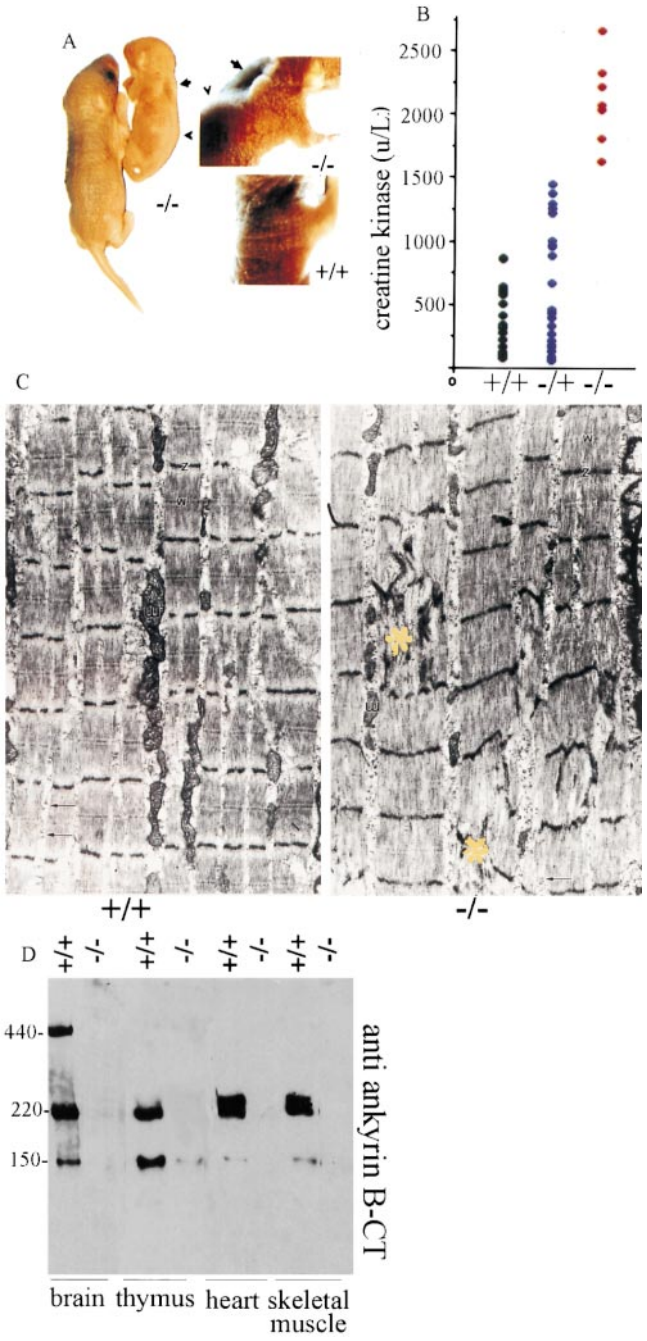

Figure 1. Musculoskeletal defects, neonatal myopathy, and loss of expression of 220- and 150-kD ankyrin-B polypeptides in striated muscle and thymus of ankyrin-B (−/−) mice. (A) Photograph of a 3-d-old ankyrin-B (−/−) mouse and a (+/+) littermate (left); higher magnification of the same mice (right). Note pronounced kyphosis (arrowhead) and winged scapula (arrow) of the (−/−) animal. (B) Serum creatine kinase activity of neonatal ankyrin-B (+/+), (+/−), and (−/−) mice. (C) Electron micrographs of skeletal muscle (quadriceps) from ankyrin-B (+/+) (left) and ankyrin-B (−/−) (right) mice (7-d-old littermates) at the same magnification. Note occasional focal disarray of Z-bands and sarcomeres (yellow asterisk) in ankyrin-B (−/−) muscle. (D) Immunoblots of brain, thymus, heart, and skeletal muscle of ankyrin-B (+/+) and (−/−) mice with rabbit affinity-purified antibody against ankyrin-B COOH terminus. Lanes with brain polypeptides were exposed one-fourth the time of lanes with other tissues.

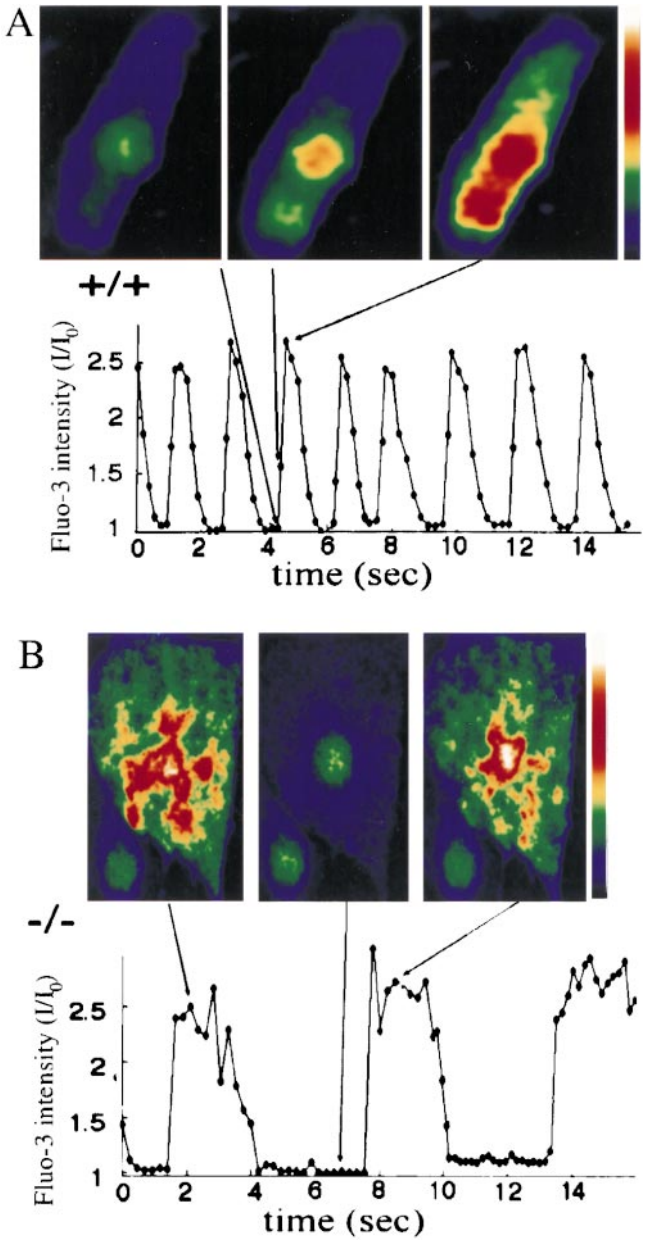

Figure 2. Abnormal spatial and temporal patterns of intracellular calcium release during spontaneous contractions of ankyrin-B (−/−) neonatal cardiomyocytes. Cytosolic Ca^{2+} levels were measured as a function of time (A and B, bottom) in cultured neonatal cardiomyocytes of littermate ankyrin-B (+/+) (A) and ankyrin-B (−/−) mice (B) using Fluo-3 as a calcium indicator (see Materials and Methods). Top panels of A and B show images of intracellular Ca^{2+} levels in cells at times indicated by lines, where the color scale on the right shows pseudocolored Ca^{2+} intensity levels, increasing from black (low Ca^{2+}) to white (high Ca^{2+}). Note that the ankyrin B (−/−) cardiomyocyte shows several distinct foci of increased Ca^{2+} levels during Ca^{2+} release (B, top left and right).

regular sinusoidal oscillation of cytosolic Ca^{2+} levels with a frequency of about 1 Hz and an increase in Ca^{2+} elevation over the basal level of ~2.5-fold (Fig. 2 A). Ankyrin-B (−/−) cardiomyocytes exhibit an irregular pattern of Ca^{2+} release with periods of prolonged elevation (average 2.5 times longer than normal) combined with a threefold reduction in frequency (Fig. 2 B). The spatial pattern of Ca^{2+} release also was abnormal in ankyrin-B (−/−) cells (Fig. 2). Wild-type cardiomyocytes exhibited one or two well resolved sites of elevated Ca^{2+} which then propagated along the cell (Fig. 2 A, top), while mutant cells exhibited multiple simultaneous foci of elevated calcium (Fig. 2 B, top).

The distribution of SR proteins involved in Ca^{2+} release and uptake was examined in ankyrin–4-B (+/+) and (−/−) cardiomyocytes maintained in culture for 4–6 d (Figs. 3 and 4) and in sections of skeletal muscle (Fig. 5). SERCA 2 (Fig. 3 A2, left) is distributed in normal cardiomyocytes in a longitudinal and cross-striated pattern coinciding with the network SR and sarcomeres, which are identified by labeling of α-actinin, a component of the Z-line (Fig. 3 A1, left). In striking contrast, SERCA 2 of ankyrin-B (−/−) cardiomyocytes is restricted to a perinuclear distribution (Fig. 3 A2, right) and is completely absent from striations associated with sarcomeres (Fig. 3 A1, right panel). The absence of SERCA 2 from contractile units of ankyrin-B (−/−) cardiomyocytes could contribute to the prolonged time of decay of Ca^{2+} transients observed in these cells (Fig. 2). SERCA 1 also is missing from sarcomeres in sections of skeletal muscle of 7-d-old ankyrin-B (−/−) mice (Fig. 5 B). Labeling for SERCA does occur along muscle fibers, but this may represent nonspecific interactions of antibodies with components of connective tissue (Fig. 5, B).

Ryanodine receptors are abnormally localized in ankyrin-B (−/−) cardiomyocytes (Figs. 3 and 4), and skeletal muscle (Fig. 5). Ryanodine receptor type 2 of normal cardiomyocytes is present in a single periodic pattern (Fig. 3 B, left) that overlays the Z-line (not shown) and corresponds to the site of T-tubules in heart cells. Ryanodine receptor type 1 in normal skeletal muscle is distributed in a periodic pattern as a double row (Fig. 5 A, left), as expected from a distribution flanking T-tubules in these cells. Ryanodine receptor type 2 in ankyrin-B (−/−) cardiomyocytes is localized in 0.5–1-μm structures dispersed throughout the cell and in a pattern distinct from striations observed in normal cells (Fig. 3 B, right). Ryanodine receptor type 1 in ankyrin-B (−/−) skeletal muscle exhibits only occasional sites of label within muscle fibers (Fig. 5 A, right). Fluorescent label for the ryanodine receptor type 1 is localized adjacent to the plasma membrane in ankyrin-B (−/−) fibers (Fig. 5 A, right), but this may represent nonspecific interactions of antibodies as noted above with SERCA.

Rescue of Abnormal Localization of SERCA and Ryanodine Receptors in Ankyrin-B (−/−) Cardiomyocytes by Transfection with cDNA Encoding 220-kD Ankyrin-B–GFP

Transfection of ankyrin-B (−/−) cardiomyocytes with cDNA encoding 220-kD ankyrin-B with a COOH-terminal green fluorescent protein (GFP) tag restored normal striated patterns of distribution of SERCA 2 (Fig. 4 C, middle) as well as ryanodine receptor type 2 (Fig. 4 G, middle). 220-kD ankyrin-B–GFP in rescued cardiomyocytes was visualized with antibody against GFP, and ex-

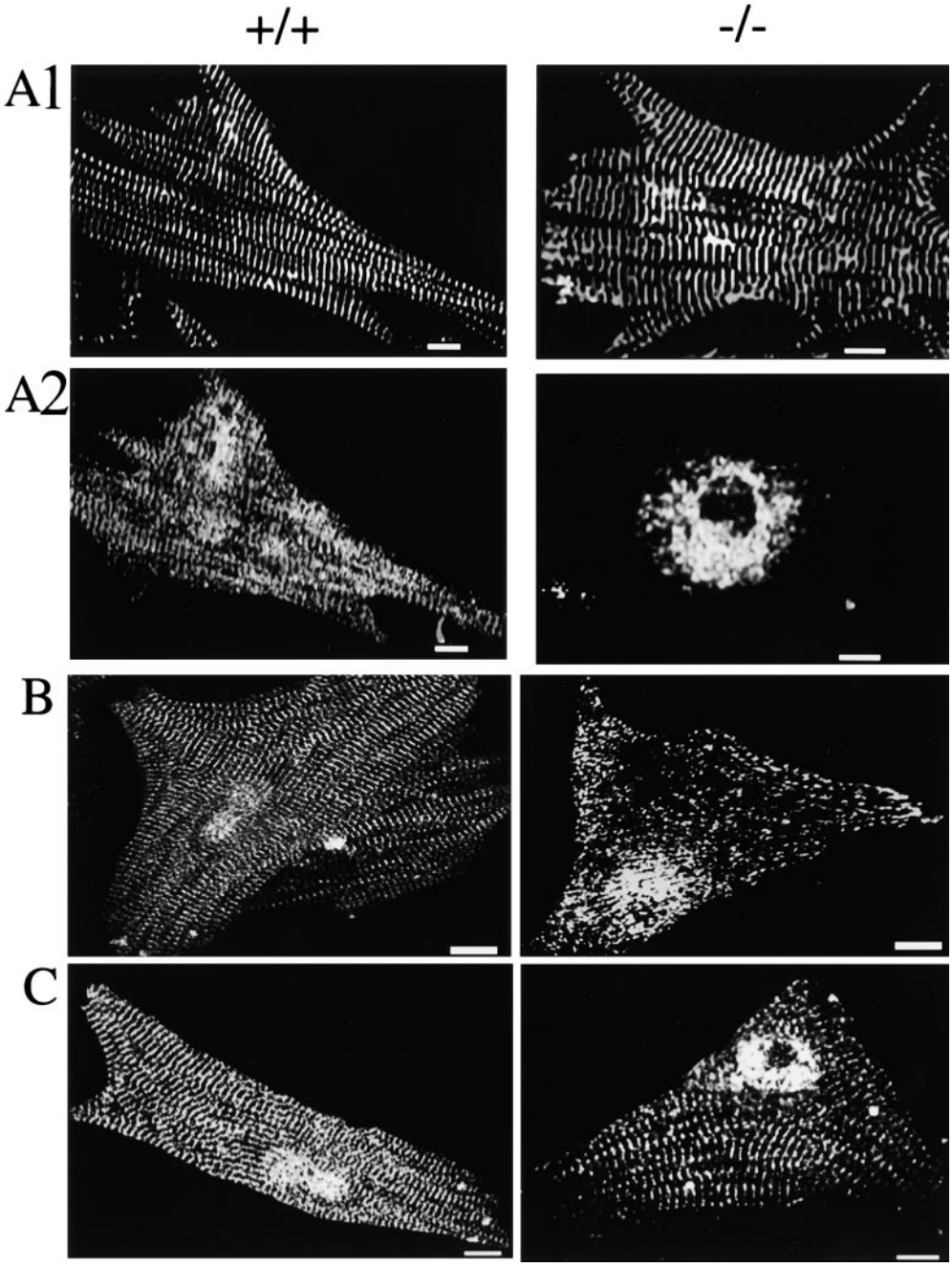

Figure 3. Neonatal cardiomyocytes of ankyrin-B (−/−) mice exhibit abnormal distribution of SR CaATPase (SERCA) and ryanodine receptors and normal localization of α-actinin and dihydropyridine receptors. A–C show immunofluorescent labeling of ankyrin-B (+/+) (left) and (−/−) (right) cardiomyocytes double-labeled with antibodies against α-actinin (A1) and SERCA 2 (A2) (A); antibodies against the ryanodine receptor type 1 and 2 (B) and antibody against the dihydropyridine receptor (voltage-sensitive calcium channel) (C). Bars, 10 μm.

hibited a striated distribution similar to that of native ankyrin-B (Fig. 4; normal in A and E; rescued in C and G). The presence of sarcomeres in these cardiomyocytes was established by labeling F-actin with biotin-phalloidin/Cy5-streptavidin (Fig. 4, A–H, left panels). Ability to restore normal organization of both SERCA 2 and ryanodine receptor type 2 with 220-kD ankyrin-B demonstrates that other ankyrin-B spliceoforms, such as the 150-kD polypeptide, are not required for this activity. Transfection with cDNA encoding 190-kD ankyrin-G–GFP did not restore SERCA 2 or ryanodine receptor type 2 patterns (Fig. 4, D and H). Moreover, 190-kD ankyrin-G–GFP was not localized in a striated pattern but instead was distributed more or less evenly throughout the cytoplasm of transfected cardiomyocytes (Fig. 4, D and H, right panels). 190-kD ankyrin-G–GFP polypeptide contains the same domains as 220-kD ankyrin-B, but has a shorter COOH-terminal domain (Zhang and Bennett, 1998). Ankyrin-G and ankyrin-B thus have distinct and nonoverlapping localizations and functions in striated muscle.

SR–T Tubule Junctions Are Preserved in Ankyrin-B (−/−) Skeletal Muscle

The abnormal localization of ryanodine receptors and SERCA in cardiomyocytes (Figs. 3 and 4) and skeletal muscle (Fig. 5) could be due either to defects in targeting of these protein to otherwise normal SR and junctional

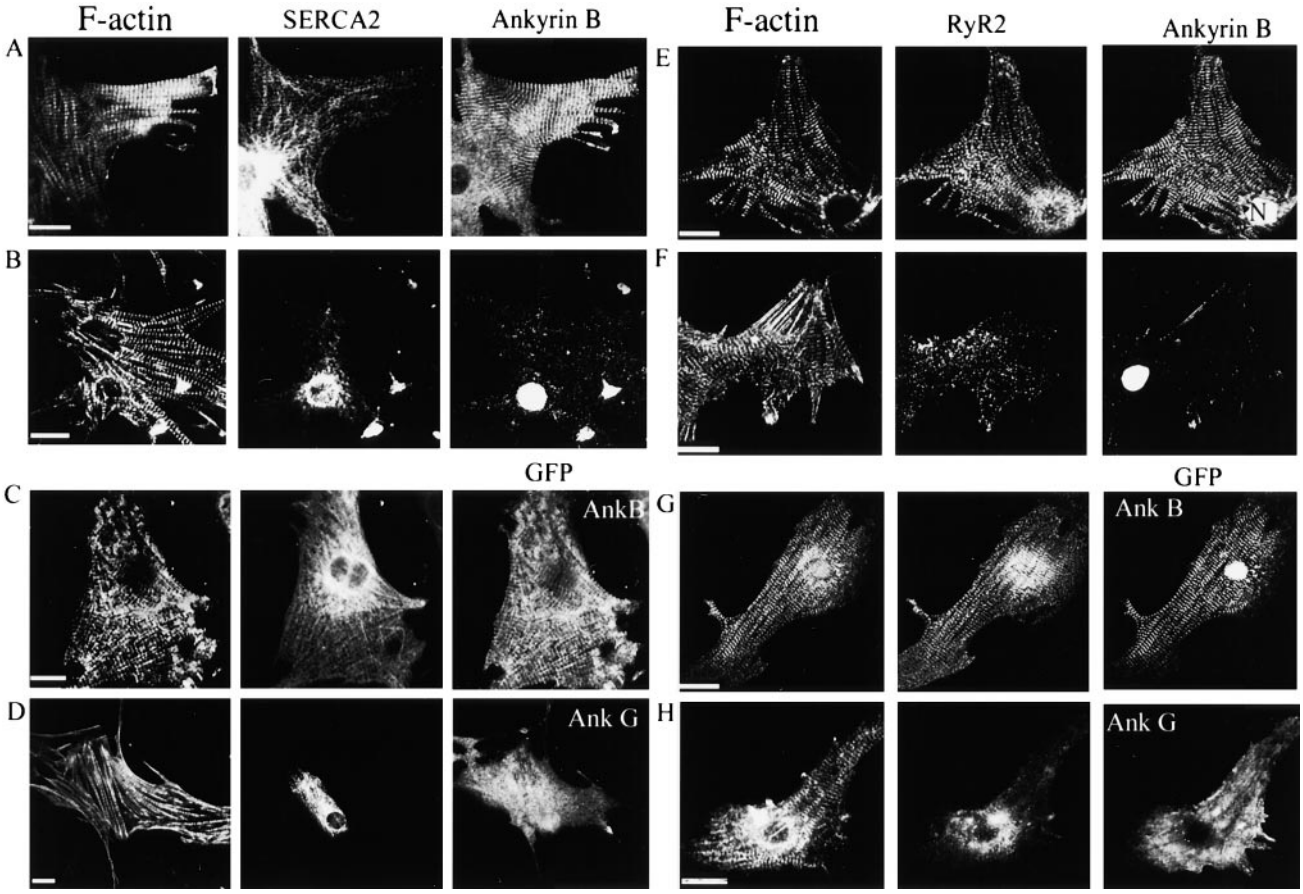

Figure 4. Rescue of abnormal localization of SERCA and ryanodine receptors in ankyrin-B (−/−) cardiomyocytes by transfection with cDNA encoding 220-kD ankyrin-B–GFP. A, B, E, and F show ankyrin-B (+/+) cardiomyocytes (A and E), and ankyrin-B (−/−) cardiomyocytes (B and F), triple-labeled for F-actin with biotin phalloidin/Cy5-labeled avidin (left panels), ankyrin-B (A, B, E, and F, right panels) and either SERCA (A and B, middle panels) or ryanodine receptor (E and F, middle panels). C, D, G, and H show ankyrin-B (−/−) cardiomyocytes transfected with cDNA encoding either 220-kD ankyrin-B–GFP (C and G), or 190-kD ankyrin-G–GFP (D and H), triple-labeled for F-actin with phalloidin (C, D, G, and H, left panels), GFP (C, D, G, and H, right panels) and either SERCA (C and D, middle panels) or ryanodine receptor (G and H, middle panels). Culture of cardiomyocytes, transfections, and immunofluorescence microscopy were performed as described in Materials and Methods. Note recovery of normal SERCA and ryanodine receptor distribution after transfection with ankyrin-B–GFP but not ankyrin-G–GFP. Bars, 20 μm.

SR sites, or to abnormal localization of the entire SR and junctional SR. Immunofluorescence using antibodies against established components of SR/T-tubule junctions and electron microscopy were used to distinguish between these possibilities.

The pattern of labeling for triadin, a SR protein associated with ryanodine receptors at SR/T-tubule junctions (Guo et al., 1994), is normal in ankyrin-B (−/−) skeletal muscle (Fig. 5 C). Moreover, labeling for the dihydropyridine receptor also is normal in skeletal muscle (Fig. 5 D) as well as cardiomyocytes (Fig. 3). These results suggest that T-tubules and the SR are present in the correct location and are linked by junctions.

Direct evidence for apparently normal SR/T-tubule junctions and SR in ankyrin-B (−/−) skeletal muscle is provided by electron micrographs (Figs. 6 and 7). Wild-type and ankyrin-B null skeletal muscles both have small T-tubules (small arrows) positioned about midway between the Z-bands (Z) and the M-lines of well-ordered sarcomeres (Fig. 6). Where the section plane is favorably oriented, the network of membranes of the longitudinal sarcoplasmic reticulum (SR) can be visualized as well-organized around the myofibrils and sarcomeres in both normal and ankyrin (−/−) fibers (Fig. 6). Junction (triads) between the T-tubule (lumen marked by t) and the SR membranes (arrows) also appear similarly well-organized overall, with the density between the SR and T-tubule membranes of the triads (arrows) equally evident in normal and ankyrin-B (−/−) fibers.

A gallery of skeletal muscle triads from normal (A–D) and ankyrin-B (−/−) (E–H) animals visualized at higher magnification are presented in Fig. 7. In both wild-type and ankyrin-B (−/−) skeletal muscle, the junctional SR (JSR) membrane forms a sac (arrowhead) abutting the T-tubule, where the JSR is seen en face. The JSR membrane is usually marked by a row of particles parallel to the junction and is frequently associated with filamentous densities extending away from the junction at right angles. The particles evident in ankyrin-B (−/−) muscle presumably are comprised of the voltage-gated calcium channel,

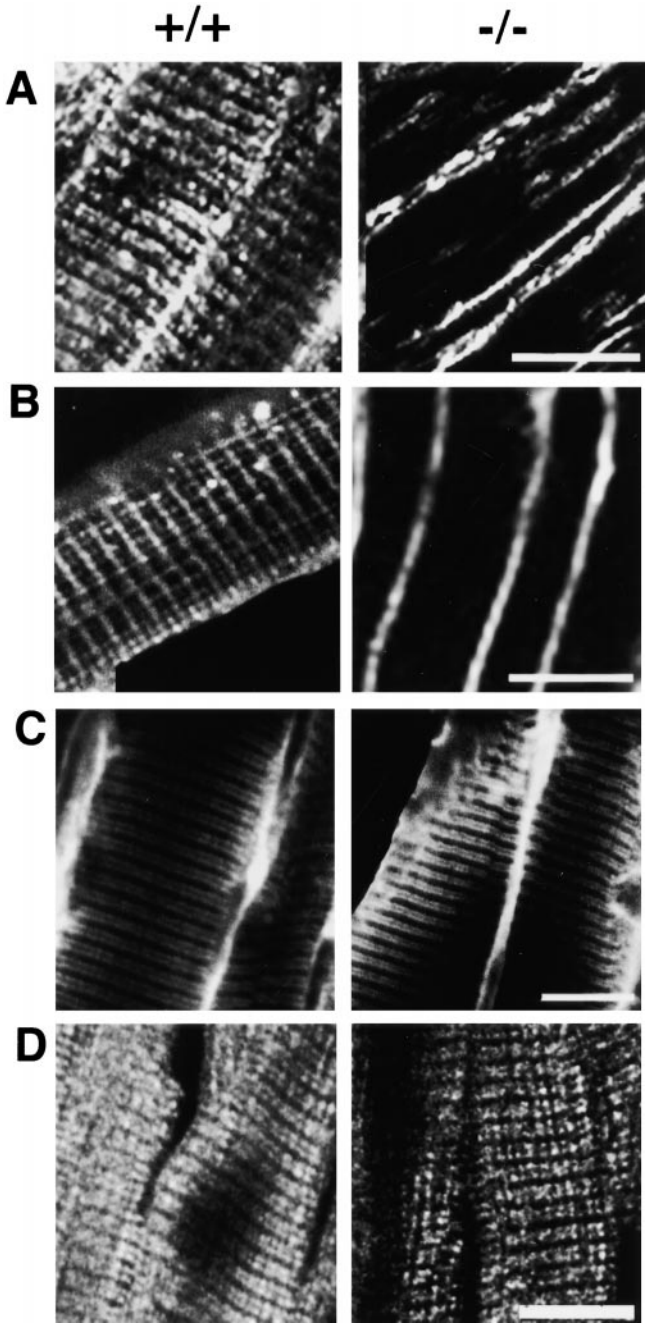

Figure 5. Normal localization of dihydropyridine receptor and the SR/T-tubule protein triadin and abnormal localization of SERCA and ryanodine receptor in ankyrin-B (−/−) skeletal muscle. A–D show longitudinal sections of skeletal muscle of ankyrin-B (+/+) (left) and (−/−) (right) 7-d-old littermate mice that are labeled with antibody against the ryanodine receptor type 1 and 2 (A), SERCA 1 (B), triadin (C), and the dihydropyridine receptor (D). Bars, 10 μm.

triadin, and perhaps other SR and/or T-tubule proteins, but not ryanodine receptor 1, which is absent based on immunofluorescence (Fig. 5 A). Measurements across 9 examples of well-oriented T-tubule–JSR membrane junctions in normal and 9 in ankyrin-B (−/−) skeletal fibers visualized at the same magnification indicated a ten percent reduction in thickness of the ankyrin-B (−/−) junctions. (The range in normal fibers was 0.9–1.1 mm [average 1.01 mm]; the range in mutant was 0.8–1.0 mm [average 0.92 mm].)

Complete absence of ryanodine receptor type 1 in the RYR1 (−/−) mouse results in loss of particles in SR–T-tubule junctions and a reduction in thickness of ~40% (Takekura et al., 1995). Retention of structures in SR–T-tubule junctions in our sections of ankyrin-B (−/−) skeletal muscle suggests that ryanodine receptors are not completely absent. One possible explanation is that ryanodine receptors are reduced in amount such that they are not evident by immunofluorescence, especially at high contrast, but are present in sufficient quantities to detect by electron microscopy.

The combined observations of normal immunofluorescent patterns of labeling of triadin and DHPR (Fig. 5) and electron microscopy (Figs. 6 and 7) strongly support the interpretation that the SR and SR–T-tubule junctions are normal overall in localization in ankyrin-B (−/−) skeletal muscle.

The reduced amount of ryanodine receptors and absence of SERCA from a normal striated pattern in ankyrin-B (−/−) skeletal muscle therefore reflects a defect in targeting of these proteins to their cellular sites. A similar conclusion also is true for heart based on electron microscopy (not shown), and the normal appearance of DHPR in cardiomyocytes (Fig. 3).

Ankyrin-B Is Not Associated in Permanent Stoichiometric Complexes with the Majority of Ryanodine Receptors or SERCA

Ankyrin-B in skeletal muscle is located in two sites that can be resolved in longitudinal (Fig. 8 A) and in transverse (Fig. 8, B and C) sections of muscle fibers. One site, visualized in an optical section along the surface of the plasma membrane, is in a costamere pattern (Craig and Pardo, 1983) at the sarcolemma, and is aligned with the Z-lines that are labeled by α-actinin (Fig. 8 A, a4–a6, green). The other location, visualized with an optical section through the interior of the fiber, is in intracellular punctate structures aligned with the A-band (Fig. 8 A, a1–a3). Transverse sections also reveal ankyrin-B staining at the sarcolemma, and in a punctate intracellular pattern (Fig. 8 B, b2 and C, c2). The pattern of ankyrin-B labeling in costameres and in intracellular sites over the A-band is distinct from the localization of ankyrin noted at T-tubules (Flucher et al., 1990). However, ankyrin-B localization does closely resemble the labeling obtained by Nelson and Lazarides (1984) with antibody raised against chicken erythrocyte ankyrin.

Double immunofluorescence labeling of transverse sections of skeletal muscle reveals that ankyrin-B is localized at sites distinct from both SERCA 1 (Fig. 8 B) and from ryanodine receptor type 1 (Fig. 8 C). The majority of SERCA1 and ryanodine receptor type 1 are clearly not in close contact with ankyrin-B (Fig. 8). Therefore, ankyrin-B cannot participate as a common structural component of the SR–T-tubule junction. Possible mechanisms involving a catalytic role of ankyrin-B in localization of ryanodine receptors and SERCA are discussed below.

Subcellular fractionation of skeletal muscle supports the idea that the punctate intracellular staining of ankyrin-B

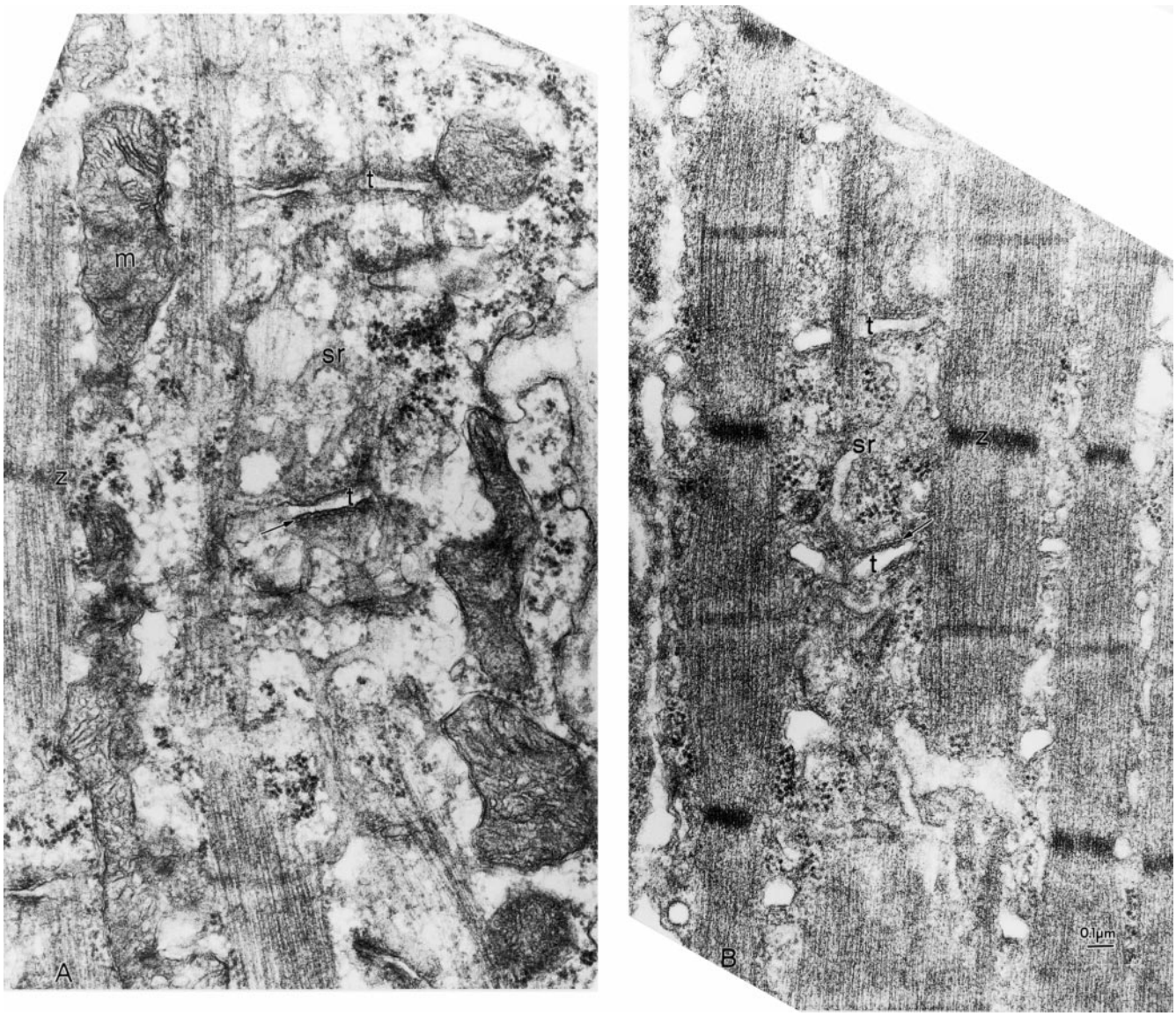

Figure 6. T-tubule and SR compartments and junctions between them are present in ankyrin-B (−/−) skeletal muscle. Electron micrographs (see Materials and Methods) of quadriceps muscle comparing the organization of the T-tubules and sarcoplasmic reticulum in littermates of normal (A) and ankyrin (−/−) (B) skeletal muscle. The T-tubule lumen is marked by t and the SR membranes by arrows. Note equivalent density between the SR and T-tubule membranes of the triads (arrows) in normal and ankyrin-B fibers.

represents vesicles (Fig. 9). The majority of 220-kD ankyrin-B pelleted after centrifugation for 10 min at 2,000 *g*, and presumably is associated with myofibrils (data not shown). However, some 220-kD ankyrin-B sedimented only at high speeds (at least 30 min at 100,000 *g*). Particulate 220-kD ankyrin-B sediments with a similar density to SERCA and ryanodine receptors after sedimentation to equilibrium in sucrose density gradients, and therefore most likely is associated with membranes (Fig. 9 B). Visualization of membrane-associated ankyrin-B by immunofluorescence microscopy revealed small structures <1 μm in diameter that presumably represent small vesicles and are distinct from vesicles labeled for SERCA (not shown).

Mislocalization of IP3 Receptors in Cardiomyocytes and Thymus of Ankyrin-B (−/−) Mice

IP3 receptors are widely expressed channels responsible for intracellular Ca^{2+} release regulated by IP3 and Ca^{2+}, and are coexpressed with ryanodine receptors in striated muscle as well as other tissues. IP3 receptors visualized by immunofluorescence are mis-sorted in ankyrin-B neonatal cardiomyocytes (Fig. 10 A). IP3 receptors in normal cardiomyocytes are distributed in a striated pattern, while in mutant cells IP3 receptors are in an irregular punctate distribution (Fig. 10 A). IP3 receptors in normal skeletal muscle are distributed in a SR pattern distinct from the pattern of ryanodine receptors, while IP3 receptors in

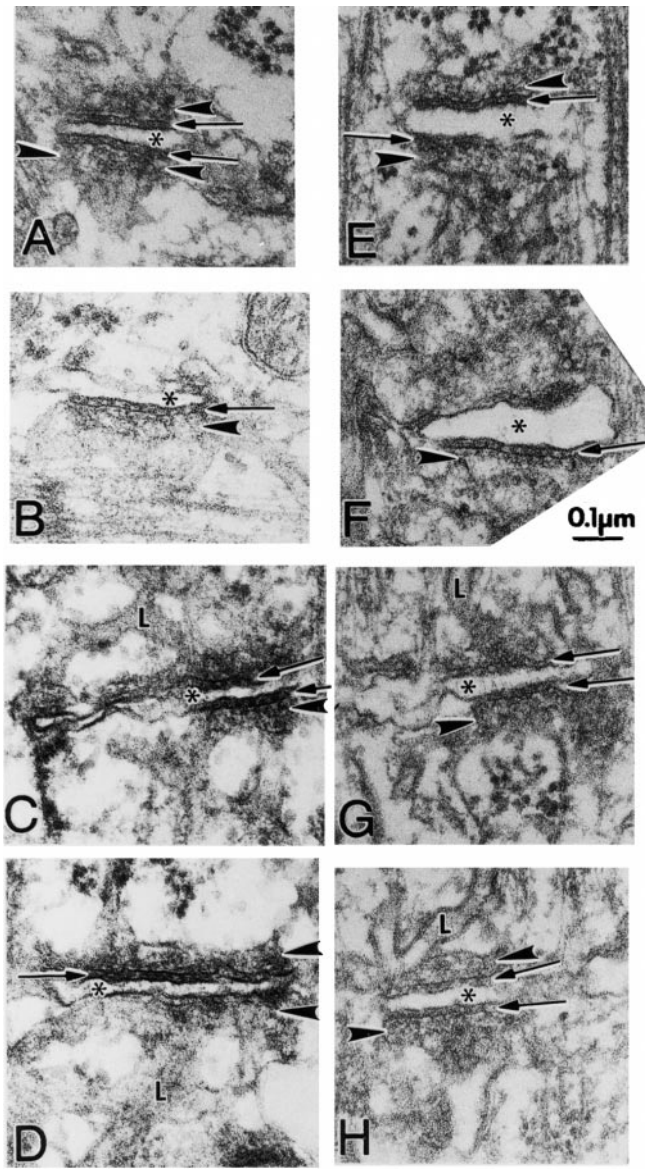

Figure 7. Triads appear structurally normal in ankyrin-B (−/−) skeletal muscle. Electron micrographs (see Materials and Methods) comparing T-tubule–SR junctions (triads) of mouse skeletal muscle from the quadriceps of normal (A–D) and ankyrin-B (−/−) (E–H) littermates at the same magnification. In both wild-type and ankyrin-B (−/−) fibers, the junctional SR (JSR) is seen more or less en face. The JSR membrane is usually marked by at least two rows of particles parallel to the junction and is frequently marked by filamentous densities extending away from the junction at right angles. The rows of particles can be seen between the arrowheads in A and opposite the arrowheads in B, C, E, F, and H. The filamentous density is best seen between arrowheads in A and opposite lower arrowheads in B, E, and F. In H, the two rows of particles appear as a jagged line (arrowhead), whereas in D and G, density on the JSR appears amorphous. Normal junctions show periodic foot processes in the gap (arrows) between T-tubule (*) and junctional SR membranes (arrowheads). Ankyrin-B (−/−) T–SR junctions show some densities between the SR and T-tubule membranes, particularly clear in (F), but the images in (E) and (H) are more common. The JSR is continuous with the tubular network of longitudinal SR (L) in both mutant and wild-type (see C, G, D, and H).

ankyrin-B (−/−) skeletal muscle are distributed throughout the cytoplasm (not shown). Levels of accumulation of IP3 receptors are reduced by at least 50% in ankyrin-B (−/−) heart tissue (Fig. 10 C).

The neonatal thymus is an active site of T cell differentiation, a process that is regulated by intracellular calcium transients mediated in part by IP3 receptors and ryanodine receptors (Crabtree and Clipstone, 1994; Guse et al., 1999). 220- and 150-kD ankyrin-B polypeptides are expressed in normal thymus (Fig. 1 D). The 220-kD polypeptide is not detectable and the 150-kD polypeptide is reduced >90% in ankyrin-B (−/−) mice (Fig. 1 D). IP3 receptors are abundantly expressed in normal thymus and are localized in a punctate perinuclear pattern in thymic lymphocytes (Fig. 10 B, left). IP3 receptors in ankyrin-B (−/−) thymus are reduced in immunoblots by ~50% (Fig. 8 C). IP3 receptors in ankyrin-B (−/−) lymphocytes also exhibit an altered pattern of localization (Fig. 10 B, right). IP3 receptors in these lymphocytes are confined adjacent to the plasma membrane, and are generally not present in the perinuclear pattern observed in normal cells (Fig. 10 B).

Reduced accumulation and abnormal localization of IP3 receptors in ankyrin-B (−/−) thymus would be anticipated to interrupt normal calcium signaling and differentiation of T cells. Consistent with such a loss of signaling, Toluidine blue–stained sections of ankyrin-B (−/−) neonatal thymus reveal cell death of a major fraction of T cells (Fig. 11). Epithelial cells are present in equivalent numbers and organization, while the majority of T cells are missing or exhibit pyknotic nuclei. In contrast, sections of normal thymus are densely populated with T cells containing normal nuclei.

Discussion

This report describes a congenital myopathy and major loss of thymic lymphocytes in ankyrin-B (−/−) mice, as well as dramatic alterations in intracellular localization of key components of the Ca^{2+} homeostasis machinery in ankyrin-B (−/−) striated muscle and thymus. The SR and SR–T-tubule junctions are apparently preserved in a normal distribution in ankyrin-B (−/−) skeletal muscle based on electron microscopy and the presence of a normal pattern of triadin and DHPR. The abnormal localization of SERCA and ryanodine receptors therefore represents a defect in intracellular sorting of these proteins in skeletal muscle. Extrapolation of these observations suggests defective targeting as the basis for abnormal localization of ryanodine receptors, IP3 receptors and SERCA in heart, and of IP3 receptors in the thymus of ankyrin-B (−/−) mice. Mis-sorting of SERCA 2 and ryanodine receptor 2 in ankyrin-B (−/−) cardiomyocytes is rescued by expression of the 220-kD ankyrin-B, demonstrating that lack of the 220-kD ankyrin-B polypeptide is the primary defect in these cells. Ankyrin-B is associated with intracellular vesicles, but is not colocalized with the bulk of SERCA 1 or ryanodine receptor type 1 in skeletal muscle. These data provide the first evidence for a physiological requirement for ankyrin-B in intracellular targeting of the calcium homeostasis machinery of striated muscle and immune system, and moreover support a catalytic role that does

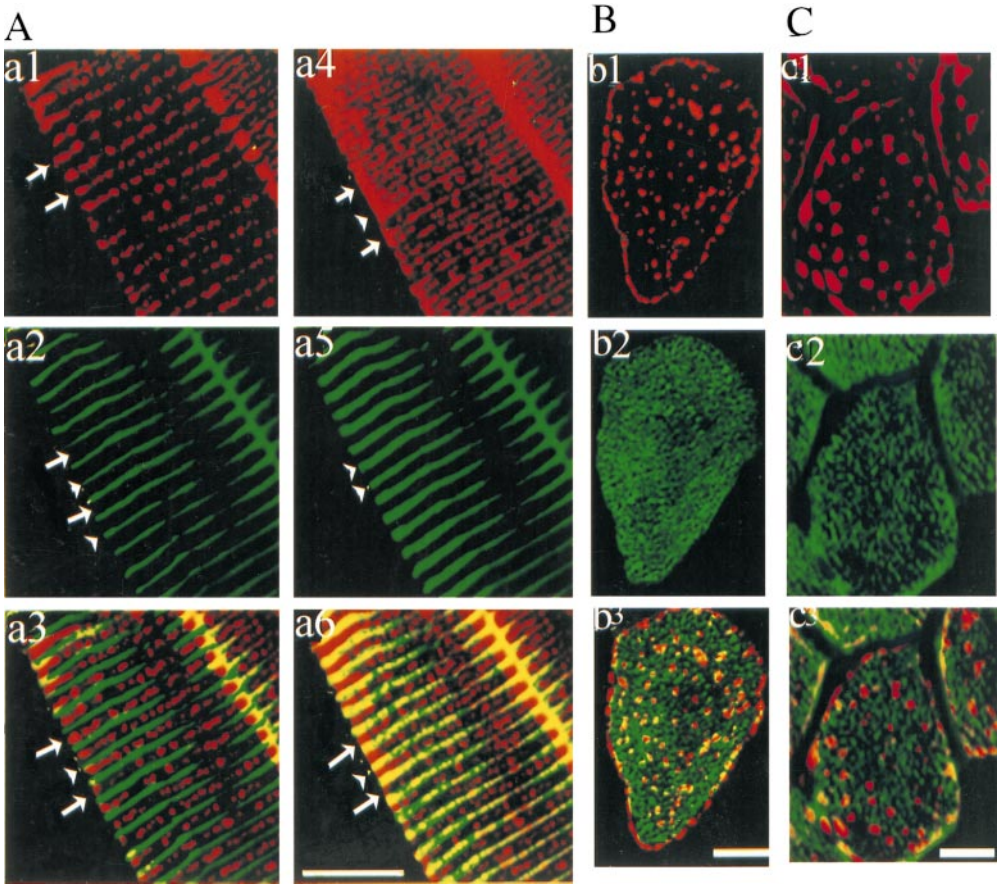

Figure 8. Ankyrin-B in skeletal muscle is localized at costameres and intracellular sites that are distinct from localization of SERCA 1 and ryanodine receptor type 1. (A). Immunolabeling of a longitudinal section of skeletal muscle with rabbit antibody against ankyrin (a1, a4, red) and a mouse monoclonal antibody against α-actinin (a2, a5, green) with a composite image (a3 and b3). Optical sections were taken at two different Z-heights: at the top, tangential to the cell surface (Z = 0 μm; a4–a6) and in the mid-region of the same cell (Z = −5 μm; a1–a3). Note that arrowheads point to location of Z line (α-actinin) and long arrows to the A-band. Note that ankyrin B labeling aligned with the Z-line appears just at the plasma membrane level (right). B and C show immunofluorescence labeling of cross-sections of skeletal muscle with rabbit antibody against the ankyrin-B (red, b1, b3, c1, and c3) and antibody against either SERCA 1 (B, green, b2 and b3) or ryanodine receptor type 1 and 2 (C, green, c2 and c3). Bars, 10 μm.

not involve permanent stoichiometric complexes between ankyrin-B and targeted proteins.

Evidence in support of some form of direct interactions of ankyrin-B with ryanodine receptors and IP3 receptors is provided by in vitro binding assays (Bourguignon et al., 1993, 1995). In addition, our laboratory has isolated IP3 receptors from cerebellum with an ankyrin-B membrane-binding domain affinity column, and determined a relatively modest K_D of 0.2 μM for ankyrin-B–IP3 receptor binding (data not shown). Such an affinity would be consistent with weak or short-lived interactions. SERCA has not been examined for ankyrin-B binding activity. However, SERCA shares overall sequence similarity with the Na/K ATPase, which does associate with ankyrin (Nelson and Veshnock, 1987).

Direct but transient interaction of Ca^{2+} homeostasis proteins with ankyrin-B could occur during transit of these proteins between the ER and the SR. Exchange of proteins between ER and Golgi is well known to involve a machinery for recruitment of specific cargo proteins into vesicles, and transfer of these vesicles between organelle compartments. A comparable system may also mediate transfer of functionally defined proteins from the ER to specialized sites within the SR. In this case, the basic defect in ankyrin-B (−/−) cells underlying mis-sorting of multiple Ca^{2+} homeostasis proteins could be a failure in some step required for segregation of these proteins and/or their transport between the ER and SR. According to this hypothesis, ankyrin-B would function as a SR-specific guide or escort using the touring metaphor for protein sorting (Herrmann et al., 1999).

Ankyrin-B is a multifunctional protein that could participate in ER protein sorting at several levels. The multivalent ankyrin membrane-binding domain could bind to and laterally segregate selected proteins within the plane of the ER membrane (Michaely and Bennett, 1995a,b). Ankyrin-B also could participate in coupling vesicles to transport systems through interactions of the spectrin-binding domain or the microtubule-association site (Davis and Bennett, 1984; DeMatteis and Morrow, 1998; Holleran and Holzbaur, 1998).

Coordinated assembly and spatial organization of Ca^{2+} release channels and SERCA within the ER is essential in cells of the immune system as well as in striated muscle. Lymphocytes encode information in the amplitude and frequency of intracellular waves of Ca^{2+} (Dolmetsch et al., 1997). Unlike the highly organized SR of striated muscle, lymphocytes are likely to have variable states of organiza-

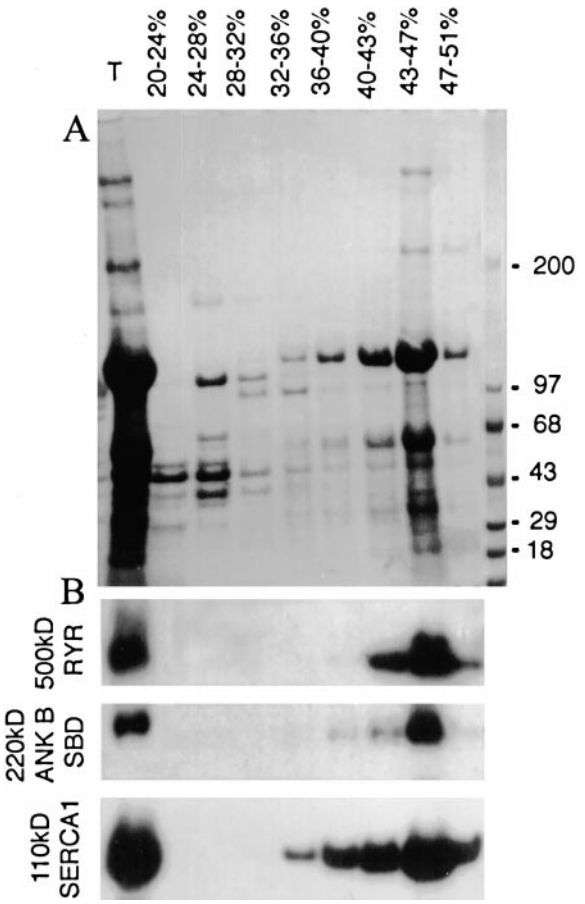

Figure 9. Ankyrin-B polypeptides in skeletal muscle are associated with a dense membrane vesicle fraction. (A) Coomassie blue–stained SDS polyacrylamide gel of starting material (T) and sucrose gradient fractions of rat skeletal muscle microsomes sedimented to equilibrium (16 h at 150,000 *g*) on a sucrose density gradient (see Materials and Methods). (B) Immunoblots of sucrose gradient fractions visualized in A using antibodies against ankyrin-B, ryanodine receptor types 1 and 2, and SERCA1.

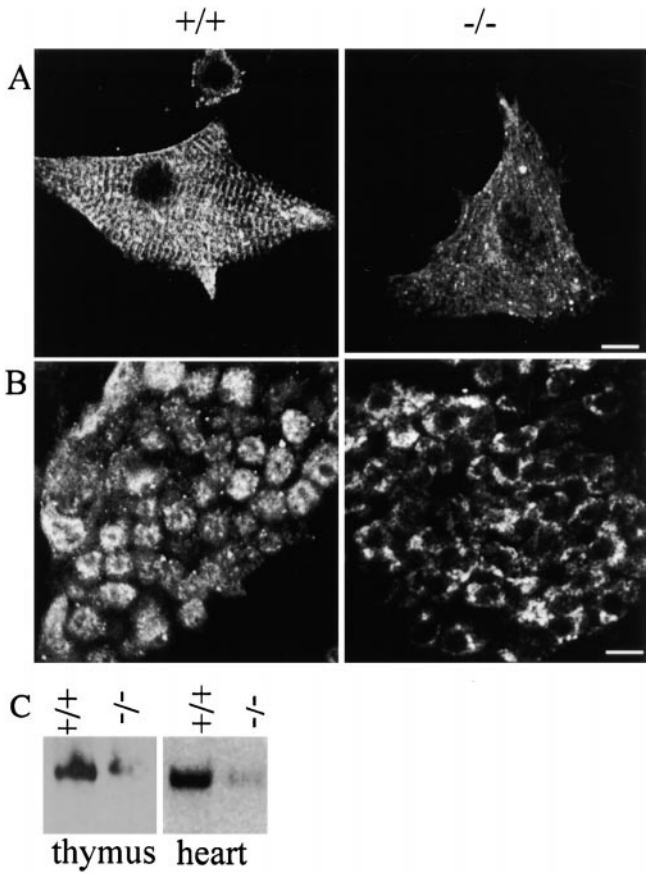

Figure 10. Abnormal localization and reduced accumulation of IP3 receptors in cardiomyocytes and thymus of ankyrin-B (−/−) mice. Cardiomyocytes (A) and sections of thymus (B) of ankyrin-B (+/+) (left) and ankyrin-B (−/−) mice are labeled with antibody against IP3 receptor (types 1, 2, and 3) and visualized by immunofluorescence. Levels of label were computationally enhanced about twofold in ankyrin-B (−/−) examples to reveal localization. C shows immunoblots of equivalent amounts of ankyrin-B (+/+) and (−/−) thymus (left) and heart (right) with antibody against the IP3 receptor. Bars: (A) 10 μm; (B) 5 μm.

tion of ryanodine receptors, IP3 receptors, and SERCA that depend on their differentiation state. As a consequence of such plasticity, signals that elevate calcium can have opposite effects in naive and differentiated cells (Dolmetsch et al., 1997). Our findings (Figs. 10 and 11) suggest that ankyrin-B is a candidate to participate in targeting IP3 receptors and possibly other Ca^{2+} homeostasis proteins to their physiological sites in T-lymphocytes. The fact that IP3 receptor accumulation is reduced in the absence of ankyrin-B also implies regulation by ankyrin-B at some level of IP3 receptor biosynthesis in addition to spatial targeting. Ankyrin-B deficiency apparently has profound consequences for survival of neonatal thymic lymphocytes (Fig. 9), as expected if signals promoting differentiation are interrupted.

The specialized neuronal ER involved in calcium homeostasis is located in dendritic spines and growth cones of axons and resembles the SR found in muscle as visualized by electron microscopy (Henkart et al., 1976). 220-kD ankyrin-B is expressed in neuron cell bodies and dendrites in the postnatal brain in a time frame that approximates development of the dendritic spine apparatus of hippocampal and Purkinje neurons (Kunimoto et al., 1991), while 440-kD ankyrin-B is targeted to axons early in development (Chan et al., 1993; Kunimoto, 1995). Although ankyrin-B (−/−) mice did not survive long enough to obtain sufficient numbers for a complete study, in two examples accumulation of IP3 receptors was significantly reduced in dendrites and cell bodies of Purkinje neurons (data not shown). These preliminary results suggest that 220-kD ankyrin-B is a good candidate to participate in targeting ER proteins dedicated to calcium homeostasis to their physiological sites in dendrites of neurons, while 440-kD ankyrin-B may have a similar function in axons.

Complete ankyrin-B deficiency in humans would be anticipated to involve defective development of the nervous system, as well as severe dysfunction of striated muscle and immune system that would not be compatible with prolonged postnatal life. However, individuals with weak alleles or partial deficiency of ankyrin-B may be viable.

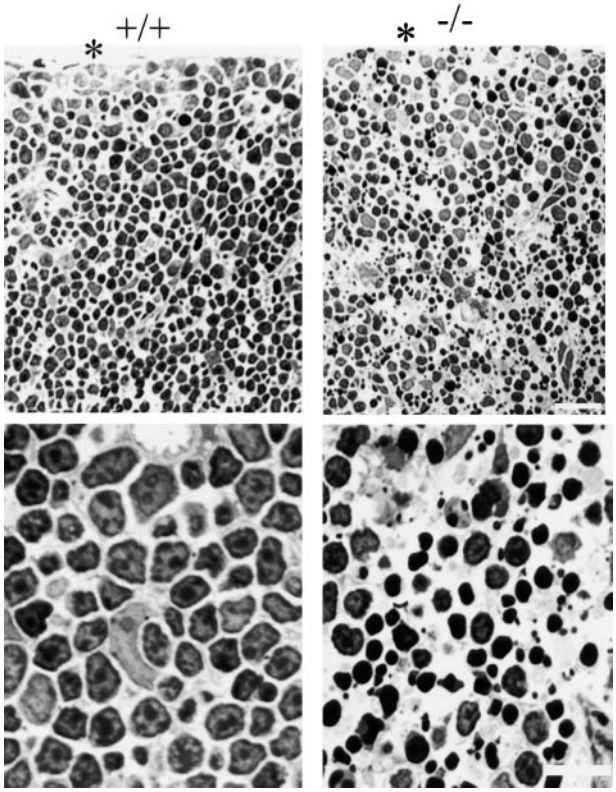

Figure 11. Toluidine blue–stained plastic sections of day 1 thymus from ankyrin-B (+/+) and (−/−) mice. Top panels are located at the cortex. An asterisk marks the margin of the thymus. Higher magnification images are shown at the bottom. Note that most of the nuclei of ankyrin-B (−/−) lymphocytes are condensed and pyknotic. Bars: (top) 25 μm; (bottom) 10 μm.

Ankyrin-B (+/−) mice have reduced expression of ankyrin-B and survive to adulthood, although with musculoskeletal defects that remain to be characterized (not shown). These animals may provide models for certain autosomal dominant human channelopathies involving Ca^{2+} release channels and SERCA, with loss of function due to mis-sorting rather than direct mutations in these proteins. For example, malignant hyperthermia, a leading cause of anesthesia-associated mortality, can be caused by mutations in the ryanodine receptor (Loke and MacLennan, 1998). However, the genetic basis for this disorder is heterogeneous, suggesting that proteins in addition to the ryanodine receptor also are involved (Robinson et al., 1998). Another candidate disease involving ankyrin-B is long QT interval type 4, an autosomal dominant cardiac arrhythmia associated with sudden death, that maps to the same chromosomal region of 4q25-27 as the ANK2 gene encoding ankyrin-B (Schott et al., 1995).

Ankyrin-G and ankyrin-R polypeptides are still expressed in the ankyrin-B (−/−) cardiomyocytes (not shown), and 190-kD ankyrin-G cannot rescue ankyrin-B (−/−) cardiomyocytes (Fig. 4). These data indicate that ankyrins, unlike many other multigene families, do not compensate for each other, and presumably have gene-specific functions. The lack of complementation between ankyrins suggests the presence of binding partners specific for each ankyrin, which have not yet been identified. Therefore, the activities proposed above for ankyrin-B in ER protein sorting are likely to involve protein interactions unique for ankyrin-B and not accessible to ankyrin-G. It will be of interest in future experiments to use chimeric ankyrins to define key domains involved in rescue of SERCA and ryanodine receptor sorting as well as cellular targeting of ankyrin-B.

Ankyrin-G and ankyrin-B both have been implicated in segregating diverse proteins within functionally defined membrane domains. However, ankyrin-G–dependent proteins are associated with specialized regions of the plasma membrane (DeMatteis and Morrow, 1998; Zhou et al., 1998), and ankyrin-B–dependent proteins are shown here to be localized in the Ca^{2+} homeostasis compartment of the ER. These parallels suggest the possibility that related mechanisms involving ankyrins but with distinct interacting proteins are responsible for restriction of proteins within certain specialized regions of plasma membrane and within the ER. A common feature of both pathways may be recognition of target proteins by ankyrin membrane-binding domains and their constituent ANK repeats. Since proteins lacking any obvious sequence homology interact with multiple distinct sites on the ankyrin membrane-binding domain (Michaely and Bennett, 1995a,b), these protein interactions are likely to result from an evolved fit mechanism rather than from targeting through a conserved sequence motif. A consequence is that evolution of ankyrin-based recognition could be driven by functional considerations of increased physiological efficiency. Other aspects of the pathways for segregation of ankyrin-dependent plasma membrane and ER proteins are also likely to be conserved, but are currently undefined. A working hypothesis for future work is that both plasma membrane and ER segregation pathways will involve formation and transport of vesicle/tubule intermediates similar to currently established communication between the ER and Golgi.

This work was funded in part by a grant from the National Institutes of Health (RO1 DK29808). Harold Erickson is thanked for his useful comments. Susan Hester is gratefully acknowledged for preparation of plastic-embedded sections of the thymus.

Submitted: 30 June 1999
Revised: 21 September 1999
Accepted: 20 October 1999

References

Beck, K.A., and W.J. Nelson. 1998. A spectrin membrane skeleton of the Golgi complex. *Biochim. Biophys. Acta.* 1404:153–160.

Beck, K.A., J.A. Buchanan, and W.J. Nelson. 1997. Golgi membrane skeleton: identification, localization and oligomerization of a 195 kDa ankyrin isoform associated with the Golgi complex. *J. Cell Sci.* 110:1239–1249.

Bennett, V., S. Lambert, J.Q Davis, and X. Zhang. 1997. Molecular architecture of the specialized axonal membrane at the node of Ranvier. *Soc. Gen. Physiol.* 52:107–120.

Berridge, M. 1998. Neuronal calcium signaling. *Neuron.* 21:13–26.

Bourguignon, L.Y., A. Chu, H. Jin, and N.R. Brandt. 1995. Ryanodine receptor-ankyrin interaction regulates internal Ca^{2+} release in mouse T-lymphoma cells. *J. Biol. Chem.* 270:17917–17922.

Bourguignon, L.Y., H. Jin, N. Iida, N.R. Brandt, and S.H. Zhang. 1993. The involvement of ankyrin in the regulation of inositol 1,4,5 trisphosphate receptor-mediated internal Ca^{2+} release from Ca^{2+} storage vesicles in mouse T-lymphoma cells. *J. Biol. Chem.* 268:7290–7297.

Chan, W., E. Kordeli, and V. Bennett. 1993. 440-kD ankyrin-B: structure of the major developmentally regulated domain and selective localization in unmyelinated axons. *J. Cell Biol.* 123:1463–1473.

Cheng, H., M.R. Lederer, R.P. Xiao, A.M. Gomez, Y.Y. Zhou, B. Ziman, H. Spurgeon, E.G. Lakatta, and W.J. Lederer. 1996. Excitation-contraction coupling in heart: new insights from Ca^{2+} sparks. *Cell Calcium*. 20:129–140.

Crabtree, G.R., and N.A. Clipstone. 1994. Signal transmission between the plasma membrane and nucleus of T lymphocytes. *Annu. Rev. Biochem*. 63: 1045–1083.

Craig, S.W., and J.V. Pardo. 1983. Gamma actin, spectrin, and intermediate filament proteins colocalize with vinculin at costameres, myofibril-to-sarcolemma attachment sites. *Cell Motil.* 3:449–462.

Davis, J., and V. Bennett. 1984. Brain ankyrin—a membrane associated protein with binding sites for spectrin, tubulin and the cytoplasmic domain of the erythrocyte anion channel. *J. Biol. Chem*. 259:13550–13559.

De Matteis, M.A., and J.S. Morrow. 1998. The role of ankyrin and spectrin in membrane transport and domain formation. *Curr. Opin. Cell Biol.* 10:542–549.

Devarajan, P., P.R. Stabach, M.A. De Matteis, and J.S. Morrow. 1997. Na,K-ATPase transport from endoplasmic reticulum to Golgi requires the Golgi spectrin-ankyrin G119 skeleton in Madin-Darby canine kidney cells. *Proc. Natl. Acad. Sci. USA*. 94:10711–10716.

Devarajan, P., V. Stabach, V. Mann, T. Ardito, M. Kashgarian, and J.S. Morrow. 1996. Identification of a small cytoplasmic ankyrin (AnkG119) in the kidney and muscle that binds beta I sigma spectrin and associates with the Golgi apparatus. *J. Cell Biol.* 133:819–830.

Dolmetsch, R., R.S. Lewis, C.G. Goodnow, and J.I. Healy. 1997. Differential activation of transcription factors induced by calcium response amplitude and duration. *Nature.* 386:855–858.

Flucher, B.E., M.E. Morton, S.C. Froehner, and M.P. Daniels. 1990. Localization of the α1 and α2 subunits of the dihydropyridine receptor and ankyrin in skeletal muscle triads. *Neuron.* 5:339–351.

Franzini-Armstrong, C., and F. Protasi. 1997. Ryanodine receptors of striated muscles: a complex channel capable of multiple interactions. *Physiol. Rev*. 77:699–729.

Guo, W., A.O. Jorgensen, and K.P. Campbell. 1994. Characterization and ultrastructural localization of a novel 90-kDa protein unique to skeletal muscle junctional sarcoplasmic reticulum. *J. Biol. Chem*. 269:28359–28365.

Guse, A.H., C.P. da Silva, I. Berg, A.L. Skapenko, K. Weber, P. Heyer, M. Hohenegger, G.A. Ashamu, H. Schulze-Koops, B.V. Potter, and G.W. Mayr. 1999. Regulation of calcium signalling in T lymphocytes by the second messenger cyclic ADP-ribose. *Nature.* 398:70–73.

Henkart, M., D.M. Landis, and T.S. Reese. 1976. Similarity of junctions between plasma membranes and endoplasmic reticulum in muscle and neurons. *J. Cell Biol*. 70:338–347.

Herrmann, J.M., P. Malkus, and R. Schekman. 1999. Out of the ER—outfitters, escorts and guides. *Trends Cell Biol*. 9:5–7.

Holleran, E.A., and E.L. Holzbaur. 1998. Speculating about spectrin: new insights into the Golgi-associated cytoskeleton. *Trends Cell Biol.* 8:26–29.

Hoock, T.C., L.L. Peters, and S.E. Lux. 1997. Isoforms of ankyrin-3 that lack the NH2-terminal repeats associate with mouse macrophage lysosomes. *J. Cell Biol.* 136:1059–1070.

Jorgensen, A.O., A.C. Shen, W. Arnold, P.S. McPherson, and K.P. Campbell. 1993. The Ca^{2+}-release channel/ryanodine receptor is localized in junctional and corbular sarcoplasmic reticulum in cardiac muscle. *J. Cell Biol.* 120:969–980.

Kordeli, E., M.A. Ludosky, C. Deprette, T. Frappier, and J. Cartaud. 1998. Ankyrin-G is associated with the postsynaptic membrane and the sarcoplasmic reticulum in the skeletal muscle fiber. *J. Cell Sci*. 111:2197–2207.

Kunimoto, M., E. Otto, and V. Bennett. 1991. A new 440-kD isoform is the major ankyrin in neonatal rat brain. *J. Cell Biol.* 115:1319–1331.

Kunimoto, M. 1995. A neuron-specific isoform of brain ankyrin, 440-kD ankyrinB, is targeted to the axons of rat cerebellar neurons. *J. Cell Biol.* 131: 1821–1829.

Loke, J., and D. MacLennan. 1998. Malignant hyperthermia and central core disease: disorders of calcium release channels. *Am. J. Med*. 104:470–486.

Meldolesi, J., and T. Pozzan. 1998. The heterogeneity of ER calcium stores has a key role in nonmuscle cell signaling and function. *J. Cell Biol.* 142:1395–1398.

Michaely, P., and V. Bennett. 1995a. The ANK repeats of erythrocyte ankyrin form two distinct but cooperative binding sites for the erythrocyte anion exchanger. *J. Biol. Chem*. 270:22050–22057.

Michaely, P., and V. Bennett. 1995b. Mechanism for binding site diversity on ankyrin. Comparison of binding sites on ankyrin for neurofascin and the Cl^{-}/$HCO3^{-}$ anion exchanger. *J. Biol. Chem*. 270:31298–31302.

Nassar, R., M.C. Reedy, and P.A.W. Anderson. 1987. Developmental changes in the ultrastructure and sarcomere shortening in the isolated rabbit ventricular myocyte. *Circ. Res.* 61:465–483.

Nelson, W.J., and P.J. Veshnock. 1987. Ankyrin binding to (Na^{++} K^{+})ATPase and implications for the organization of membrane domains in polarized cells. *Nature.* 328:533–536.

Nelson, W.J., and E. Lazarides. 1984. Goblin (ankyrin) in striated muscle: identification of the potential membrane receptor for erythroid spectrin in muscle cells. *Proc. Natl. Acad. Sci. USA*. 81:3292–3296.

Robinson, R., J.L. Curran, W.J. Hall, P.J. Halsall, P.M. Hopkins, A.F. Markham, A.D. Stewart, S.P. West, and F.R. Ellis. 1998. Genetic heterogeneity and HOMOG analysis in British hyperthermia families. *J. Med. Genet. B*. 35:196–201.

Reedy, M.K., and M.C. Reedy. 1985. Rigor crossbridge structure in tilted single filament layers and flared-X formations from insect flight muscle. *J. Mol. Biol.* 185:145–176.

Schott, J.J., F. Charpentier, S. Peltier, P. Foley, E. Dourin, J.B. Bouhour, G. Vergnaud, L. Bachner, J.P. Moisan, P. Donnelly, et al. 1995. Mapping of a gene for long QT syndrome to chromosome 4q25-27. *Am. J. Hum. Genet.* 57: 1114–1122.

Scotland, P., D. Zhou, H. Benveniste, and V. Bennett. 1998. Nervous system defects of ankyrin-B (−/−) mice suggest functional overlap between the cell adhesion molecule L1 and 440 kD ankyrin-B in premyelinated axons. *J. Cell Biol.* 143:1305–1315.

Takekura, H., M. Nishi, T. Noda, H. Takeshima, and C. Franzini-Armstrong. 1995. Abnormal junctions between surface membrane and sarcoplasmic reticulum in skeletal muscle with a mutation targeted to the ryanodine receptor. *Proc. Natl. Acad. Sci. USA*. 92:3381–3385.

Vertel, B.M., L.M. Walters, and D. Mills. 1992. Subcompartments of the endoplasmic reticulum. *Semin. Cell Biol*. 3:325–341.

Zhang, X., and V. Bennett. 1998. Restriction of 480/270-kD ankyrin-G to axon proximal segments requires multiple ankyrin-G–specific domains. *J. Cell Biol.* 142:1571–1581.

Zhou, D., C.S. Birkenmeier, M.W. Williams, J.J. Sharp, J.E. Barker, and R.J. Bloch. 1997. Small, membrane-bound, alternatively spliced forms of ankyrin 1 associated with the sarcoplasmic reticulum of mammalian skeletal muscle. *J. Cell Biol.* 136:621–631.

Zhou, D., S. Lambert, P.L. Malen, S. Carpenter, L.M. Boland, and V. Bennett. 1998. Ankyrin-G is required for clustering of voltage-gated Na channels at axon initial segments and for normal action potential firing. *J. Cell Biol.* 143: 1295–1304.